

1 **Combined influence of oceanic and atmospheric circulations on Greenland Sea Ice** 2 **concentration**

3 Sourav Chatterjee^{1,2*}, Roshin P Raj³, Laurent Bertino³, Sebastian H. Mernild³, Subeesh MP¹, Nuncio Murukesh¹, Muthalagu

4 Ravichandran¹

5

6¹National Centre for Polar and Ocean Research, Ministry of Earth Sciences, India

7²School of Earth, Ocean and Atmospheric Sciences, Goa University, India

8³Nansen Environmental and Remote Sensing Center and Bjerknes Centre for Climate Research, Bergen, Norway

9

10 *Corresponds to:* Sourav Chatterjee (sourav@ncpor.res.in)

11

12 **Abstract.**

13 The amount and spatial extent of Greenland Sea (GS) ice are primarily controlled by the sea ice export across the Fram Strait
14 (FS) and by local seasonal sea ice formation, melting, and sea ice dynamics. In this study, using satellite passive microwave
15 sea ice observations, atmospheric and a coupled ocean-sea ice reanalysis system, TOPAZ4, we show that both the
16 atmospheric and oceanic circulation in the Nordic Seas (NS) act in tandem to explain the SIC variability in the south-western
17 GS. Northerly wind anomalies associated with anomalous low SLP over the NS reduce the sea ice export in the south-
18 western GS due to westward Ekman drift of sea ice. On the other hand, the positive wind stress curl strengthens the cyclonic
19 Greenland Sea Gyre (GSG) circulation in the central GS. An intensified GSG circulation may result in stronger Ekman
20 divergence of surface cold and fresh waters away from the south-western GS. Both of these processes can reduce the
21 freshwater content and weaken the upper ocean stratification in the south-western GS. At the same time, warm and saline
22 Atlantic Water (AW) anomalies are recirculated from the FS region to south-western GS by a stronger GSG circulation.
23 Under a weakly stratified condition, enhanced vertical mixing of these subsurface AW anomalies can warm the surface
24 waters and inhibit new sea ice formation, further reducing the SIC in the south-western GS.

251 Introduction

26The freshwaters in the GS plays an important part for Nordic Seas overflow (Huang et al., 2020), which constitutes the lower
27limb of the Atlantic meridional overturning circulation (Chafik and Rossby 2019). The freshwater content in this region is
28largely driven by the amount of sea ice therein (Aagaard & Carmack 1989). Sea ice in GS is also important in determining
29shipping routes (Instanes et al. 2005; Johannessen et al. 2007), as well as to the regional marine ecosystem due to its impact
30on the light availability (Grebmeier et al. 1995). Most of the sea ice in the GS is exported from the central Arctic Ocean
31across the Fram Strait (FS) and is largely controlled by the ice-drift with the Transpolar Drift (Zamani et al. 2019).
32Anomalous sea ice export through the FS is associated with events like the ‘Great Salinity Anomaly’ (Dickson et al. 1988)
33which can have impact on the freshwater content in the Nordic Seas. Therefore, it is quite evident that the changes in sea ice
34export through the FS influence the GS sea ice and thus the freshwater availability in the Nordic Seas (Belkin et al. 1998;
35Dickson et al. 1988; Serreze et al. 2006).

36Even though it is one of the main mechanisms contributing to the overall SIC in GS, the relation between sea ice export
37through FS and SIC variability in GS is not very robust (Kern et al. 2010). This further points to the importance of local sea
38ice formation and sea ice dynamics in the GS. The impact of these processes can be realized prominently in the marginal ice
39zone (MIZ) in the south-western GS and the ‘Odden’ region in central GS (see Fig. 1 for approximate locations of the
40regions). These regions exhibit strong negative SIC trends during recent decades (Rogers and Hung, 2008, see also Fig. 1a in
41Selyuzhenok et al. 2020). Changes in sea ice of this region can modify the deep water convection through influencing both
42the heat and salt budgets (Shuchman et al. 1998). Selyuzhenok et al. (2020) found that in spite of increasing sea ice export
43through the FS, the overall sea ice volume (SIV) in the GS has been decreasing during the period 1979–2016. They further
44attributed the interannual variability and decreasing trend of SIV to local oceanic processes, more precisely warmer AW
45temperatures in the Nordic Seas. Further local meteorological parameters e.g. air temperature, wind speed and direction
46along with oceanic waves, eddies have also been found to influence the sea ice properties in the central GS, particularly for
47the Odden region (Campbell et al. 1987; Johannessen et al. 1987; Wadhams et al. 1996; Shuchman et al. 1998; Toudal 1999;
48Comiso et al., 2001).

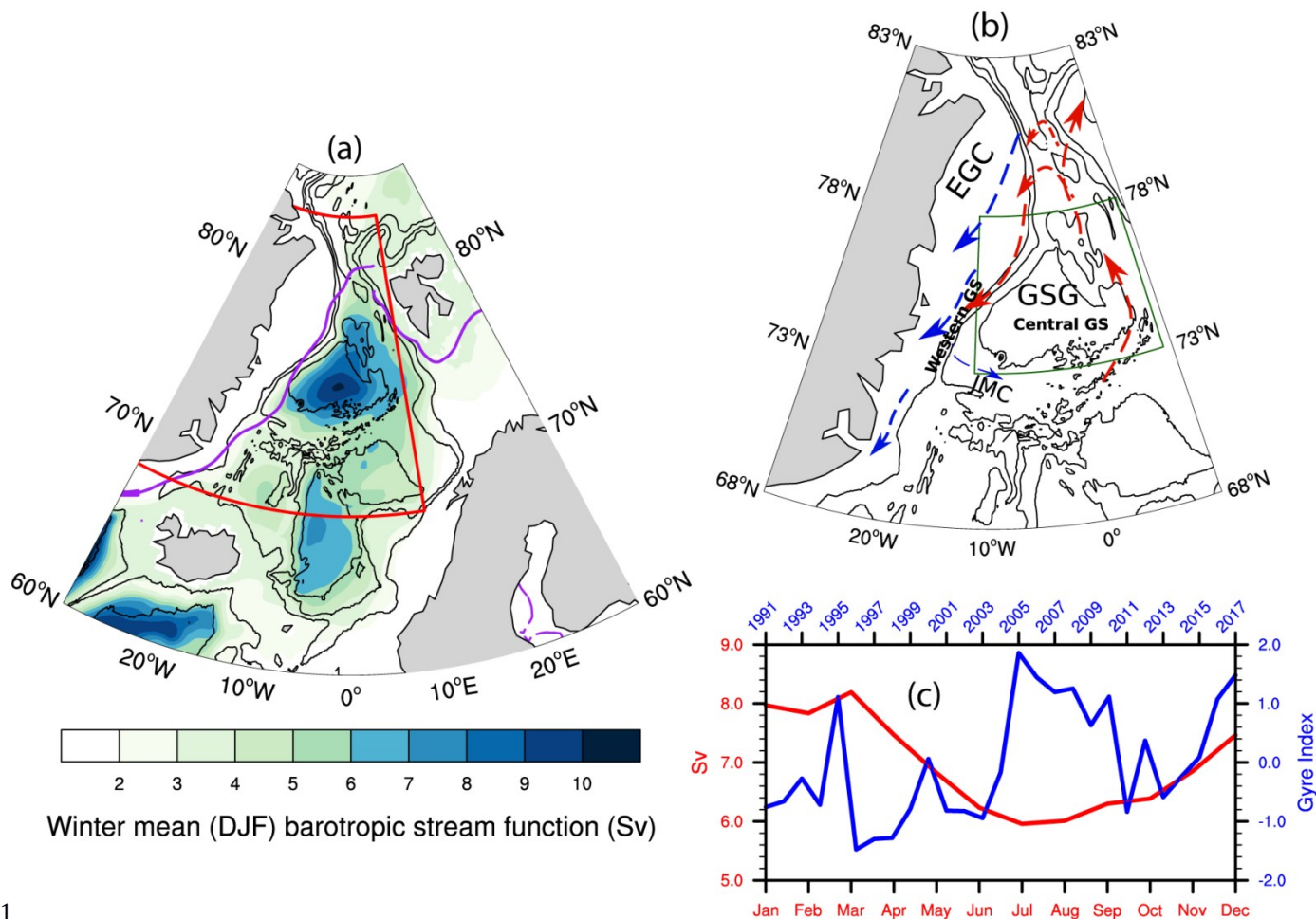
49Besides the local factors, sea ice in the GS also responds to large-scale atmospheric forcing. For example, a high sea level
50pressure (SLP) anomaly over the NS results in anomalous southerly wind in the GS. The associated Ekman drift towards the
51central GS may assist the eastward expansion of the sea ice and SIC increase in the central GS (Germe et al. 2011).
52Selyuzhenok et al. (2020) also argued that consistent positive North Atlantic Oscillation (NAO) forcing in recent decades
53have led to warmer AW in the Nordic Seas and resulted in a declining sea ice volume trend. However, the response of
54Nordic Seas circulation to the atmospheric forcing and the mechanism through which it can influence the SIC in GS is not
55studied in detail.

56

57The Greenland Sea Gyre (GSG) is a prominent large-scale feature of the Nordic Seas circulation and can be identified as a
58cyclonic circulation in the central GS basin (Fig. 1). It is known to respond to the atmospheric forcing in the NS and
59contribute to AW heat distribution in the Nordic Seas (Hatterman et al. 2016; Chatterjee et al. 2018). A stronger GSG
60circulation increases the AW temperature in the FS by modifying the northward AW transport in its eastern side (Chatterjee
61et al. 2018). A simultaneous increase in its southward flowing western branch, constituting the southern recirculation
62pathway of AW (Hattermann et al. 2016; Jeansson et al. 2017), can increase the heat content in the south-western GS
63through a stronger and warmer recirculation of AW (Chatterjee et al. 2018). The return AW, even after significant
64modification, remains denser than the local cold and fresh surface waters and thus mostly remain in the subsurface
65(Schlichtholz & Houssais 1999; Eldevik et al. 2009). However, enhanced vertical winter mixing can cause warming of the
66surface waters in the GS (Våge et al., 2018). Further, the eastward flowing Jan Mayen Current (JMC), originated from the
67East Greenland Current (EGC), constitutes the south-western closing branch of the cyclonic GSG circulation in the GS (Fig.
681b). The east-ward extension of the cold and fresh JMC into the central GS basin helps in both new sea ice formation and
69advection of sea ice from the EGC (Wadhams & Comiso 1999). Changes in GSG circulation and associated AW
70recirculation in GS may also influence the JMC strength and temperature. Thus given the potential role of GSG in modifying
71the oceanic conditions, it is important to understand how the response of GSG circulation to the atmospheric forcing can
72influence the SIC in the GS.

73

74In this study we hypothesize that the interannual winter mean SIC variability in GS can be explained by the combined
75influence of atmospheric and oceanic circulations, more precisely the GSG circulation. Using a combination of satellite
76passive microwave SIC, a coupled sea ice ocean reanalysis and atmospheric reanalysis data, we show that changes in the
77GSG dynamics and resulting AW transport in GS can potentially influence the SIC in the south-western GS. Further, we also
78show that the atmospheric circulation associated with the GSG circulation variability provides the favourable conditions for
79the GSG's control on the SIC variability in the south-western GS region. Section 2 describes the data and methods applied in
80the study following the results in section 3. Discussions and conclusions are mentioned in section 4.



81

82

83 **Figure 1:** a) Winter mean (DJF) barotropic stream function for the period 1991–2017. The region marked in red indicates
 84 the Nordic Seas region. The purple line shows the mean DJF sea ice extent for the study period. b) Schematic of the major
 85 currents and discussed in the text. JMC: Jan Mayen Current; EGC: East Greenland Current; GSG: Greenland Sea Gyre.
 86 Warm currents are drawn in red and cold currents are in blue. Black contours are showing bottom topography drawn at every
 87 1000 m. The thick black contour indicates the 3000m isobath. The marked region in dark green is used to calculate the ‘gyre
 88 index’ as detailed in the next section. c) The blue line indicates the gyre index used in this study and the red line shows the
 89 annual cycle of the strength of GSG circulation determined by averaging barotropic stream function within the 3000m
 90 isobath in the region marked in (b).

912. Data

922.1 Atmospheric data:

93 Monthly mean sea level pressure (SLP) data was obtained from the ERA Interim reanalysis (Dee et al. 2011) for the period
94 1991–2017 on a 0.5 by 0.5 degree grid resolution. Monthly anomalies were calculated from the monthly climatology field
95 using the full time period (1991–2017) and were averaged for December-January-February (DJF). For the linear regression
96 analysis the DJF averaged SLP anomalies were detrended.

97

982.2 Oceanic data:

99 Monthly mean oceanic data used in this study were taken from TOPAZ4, a coupled ocean and sea ice data assimilation
100 system for the North Atlantic and the Arctic. TOPAZ4 is based on the Hybrid Coordinate Ocean Model (HYCOM, with 28
101 hybrid z-isopycnal layers at a horizontal resolution of 12 to 16 km in the Nordic Seas and the Arctic) and Ensemble Kalman
102 Filter data assimilation, the results of which have been evaluated in earlier studies (Lien et al. 2016; Xie et al. 2017;
103 Chatterjee et al. 2018; Raj et al. 2019). TOPAZ4 represents the Arctic component of the Copernicus Marine Environment
104 Monitoring Service (CMEMS) and is forced by ERA Interim reanalysis and assimilates (every week) observations from
105 different platforms. The detailed setup and performance of the TOPAZ4 reanalysis, including the counts of observations and
106 the temporal variations of the data counts are described in Xie et al. (2017). Of particular relevance for GS are the
107 assimilation of Argo profiles, research cruises CTDs from Institute of Oceanology Polish Academy of Science (IOPAS) and
108 Alfred-Wegener Institute (AWI) (Sakov et al. 2012), satellite sea ice concentration, sea surface temperature and sea level
109 anomaly from the CMEMS platforms.

110

1112.3 Sea ice data:

112 Monthly mean sea ice concentrations (SIC) from Nimbus-7 SMMR and DMSP SSM/I-SSMIS Passive Microwave Data,
113 Version 1 (Cavalieri et al. 1996) were obtained from the National Snow and Ice Data Centre for the period 1991–2017. The
114 dataset provides a continuous time series of SIC on a polar projection at a grid scale size of 25km by 25km. Sea ice velocity
115 data was taken from the Polar Pathfinder Daily 25 km EASE-Grid Sea Ice Motion Vectors (Tschudi et al. 2019).

116

1172.4 Methods and Evaluation of TOPAZ4

118 We estimated the strength of the GSG circulation by area-averaging the winter-mean (DJF) barotropic stream function
119 anomalies within the 3000m isobath in the region 73 N:78 N; 12 W:9 E (as marked with green box in Fig. 1b). The area-
120 averaged values were then standardized over the complete time period 1991–2017 to estimate the ‘gyre index’ (Fig. 1c). In
121 this study we focused only on the winter (DJF) season as the local sea ice in GS can only form during winter and also the
122 strength of the GSG circulation peaks during winter (Fig. 1c). Composite analysis of DJF mean potential temperature
123 anomaly was performed by averaging the same for strong and weak gyre index years which were determined when the gyre

124index crosses the 0.75 and -0.75 mark respectively. The 0.75 threshold was chosen to consider only the sufficiently
125strong/weak gyre circulation periods. Throughout the article, all regression and correlation analysis were performed with the
126detrended time series for the corresponding variables. Freshwater content was calculated using the following formula

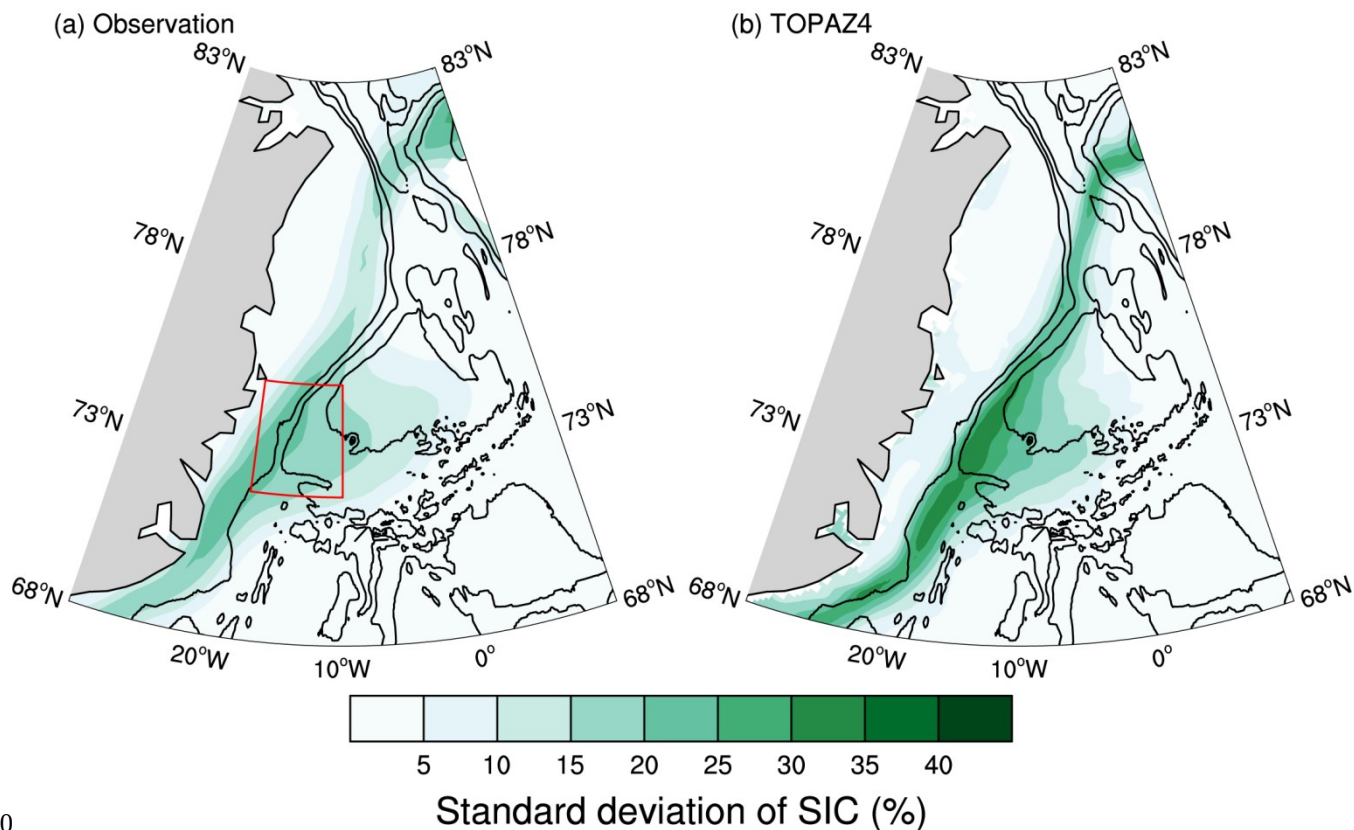
127

$$\int_z^{surf} \frac{S_{ref} - S}{S_{ref}} dz$$

128where, S is salinity and the reference salinity S_{ref} is chosen as 34.8 psu.

129

130The standard deviation of winter-mean DJF SIC, in both observation and TOPAZ4, showed high variability along the MIZ in
131south-western GS and the Odden region in central GS (Fig. 2). Note that, the TOPAZ4 reanalysis data exhibits a more
132confined MIZ than observations, which is a known model deficiency (Sakov et al. 2012). The sea ice model (Hunke and
133Dukowicz, 1997), used in TOPAZ4, has a narrower transition zone between the pack ice and the open ocean. Although
134assimilation of the sea ice observations does slightly improve the position of MIZ in TOPAZ4 compared to observation, the
135sharp transition in a narrow band still remains, which could have resulted in higher standard deviations in a narrow MIZ of
136TOPAZ4 as observed in Fig. 2b. However, as we will find in the next section, the sea ice response to the atmospheric and
137oceanic processes explained in the study can be significantly found in both the observation and TOPAZ4 with slightly higher
138signals along the MIZ in TOPAZ4. Thus the higher signal-to-noise ratio in TOPAZ4 should not affect the qualitative aspects
139of the processes and their influence on SIC, which is the main objective of the study.



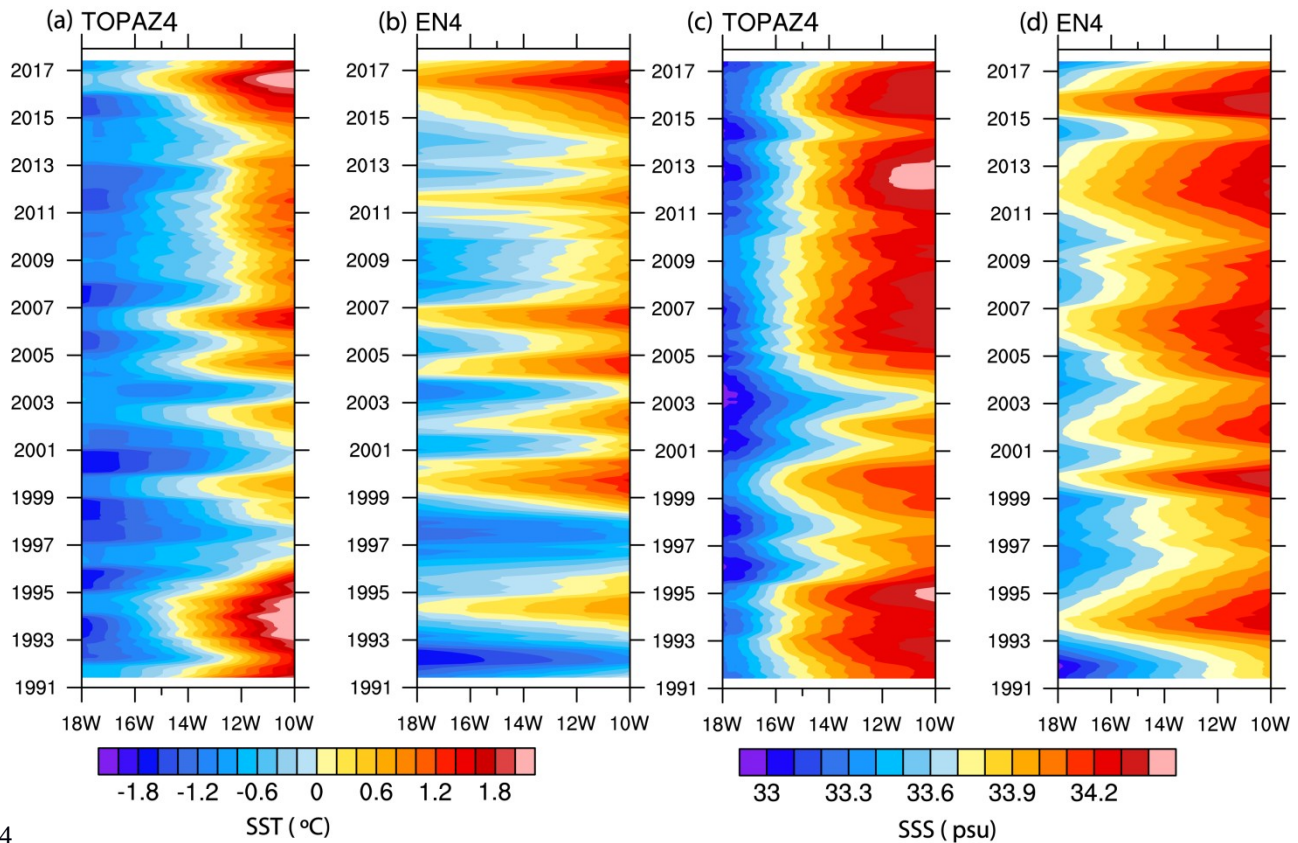
140

141

142 **Figure 2:** Standard deviations of DJF monthly mean sea ice concentration for the period 1991–2017 from (a) satellite
 143 observations (b) TOPAZ4 reanalysis. The red box with high values is drawn over the region 72N:75N; 18W:10W and is
 144 referred to as south-western GS hereafter.

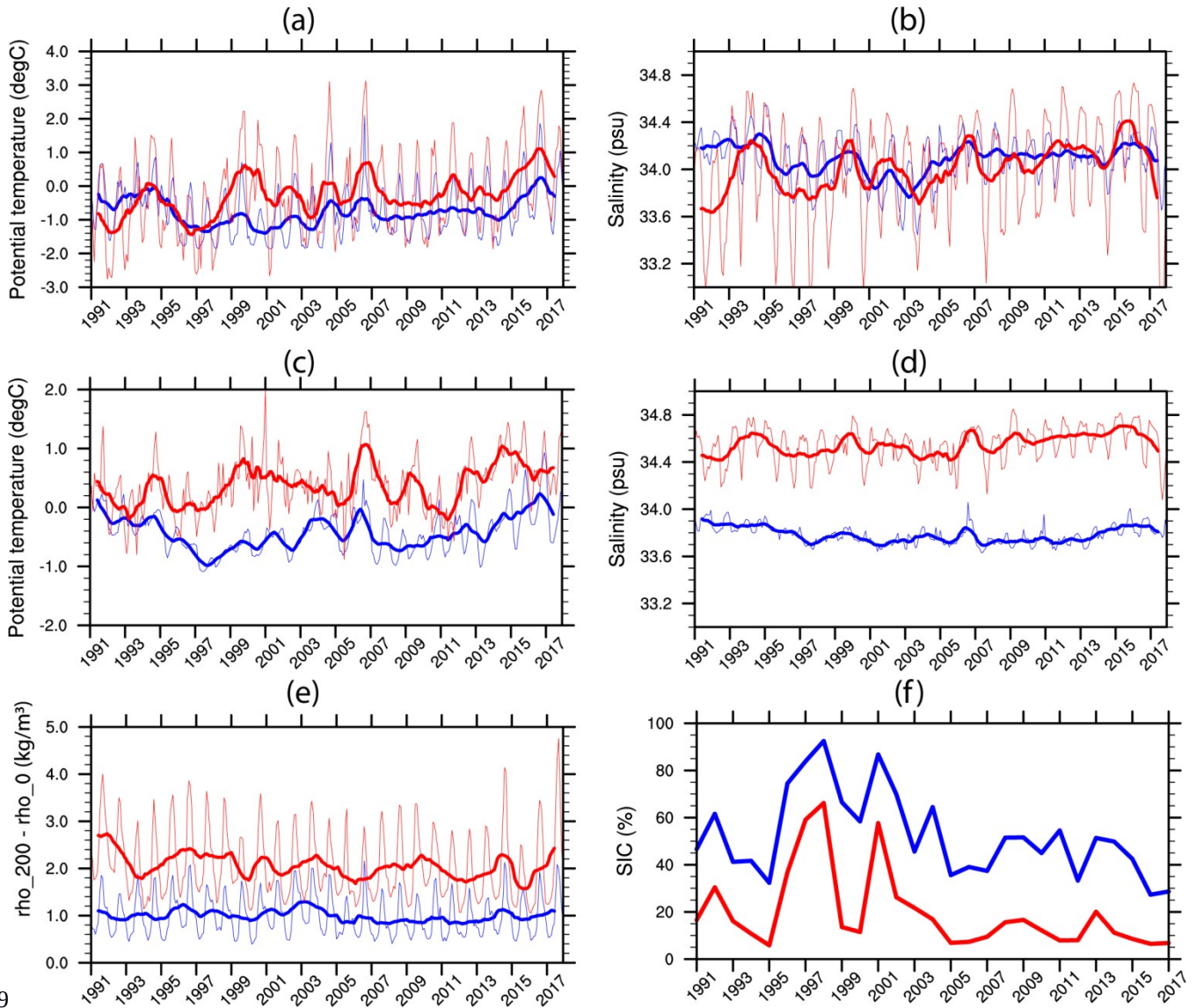
145 For evaluation of the oceanic conditions in TOPAZ4 we used temperature and salinity observations obtained from EN4
 146 (version 4.2.1) quality controlled analyses with Levitus et al. (2009) corrections applied. Here we chose to compare the
 147 oceanic parameters in a region (as marked in Fig. 2) in south-western GS where the standard deviation of the SIC is found to
 148 be maximum both in TOPAZ4 and observations. Also we will show in the next section that SIC response to the processes
 149 described here is most profound in this region. Hereafter we refer to this region as south-western GS for simplicity. Fig. 3
 150 shows the spatio-temporal patterns of sea surface temperature (SST) and salinity (SSS) in south-western GS as found in
 151 TOPAZ4 and EN4. Although the temporal evolution of these parameters are well captured in TOPAZ4, compared to
 152 observation, the westward extension of the warm and saline waters was found to be less in TOPAZ4. This indicates that the
 153 front between the cold and fresh waters along the Greenland shelf and the warm and saline waters in the south-western GS is
 154 slightly shifted towards the east in TOPAZ4 compared to observation. This could be a reason for the fact that higher standard

155 deviation of SIC is found slightly toward the east in TOPAZ4 than observations (Fig. 2). In south-western GS, both the
 156 surface and subsurface temperature in TOPAZ4 was found to be colder compared to observations (Fig. 4). The negative
 157 biases in TOPAZ4 were more profound in the subsurface for both temperature and salinity. Xie et al., (2017) also found a
 158 similar result with TOPAZ4 and attributed it to sparse observations. Using the potential density difference between 200m
 159 and the surface as an indicator of the stratification, we found that TOPAZ4 has weaker stratification compared to
 160 observations (Fig. 4e). Consistent with the cold bias in TOPAZ4, winter-mean SIC in TOPAZ4 is higher than the satellite
 161 observation in the south-western GS (Fig. 4f). However, we found a strong correlation ($r=0.9$) between the SIC in
 162 observation and TOPAZ4. This indicates that the interannual variability of SIC, which is the focus of the study, is quite
 163 consistent in both TOPAZ4 and observation.



164

165 **Figure 3:** Hovmoller (longitude-time) diagram of the SST ($^{\circ}\text{C}$; a,b) and SSS (psu; c,d) over the region over 72 N:75 N; 18
 166 W:10 W in the south-western GS as marked in Fig. 2. (a) and (c) are for TOPAZ4 and (b) and (d) for EN4 observations. In
 167 all cases data were smoothed with one year running mean.



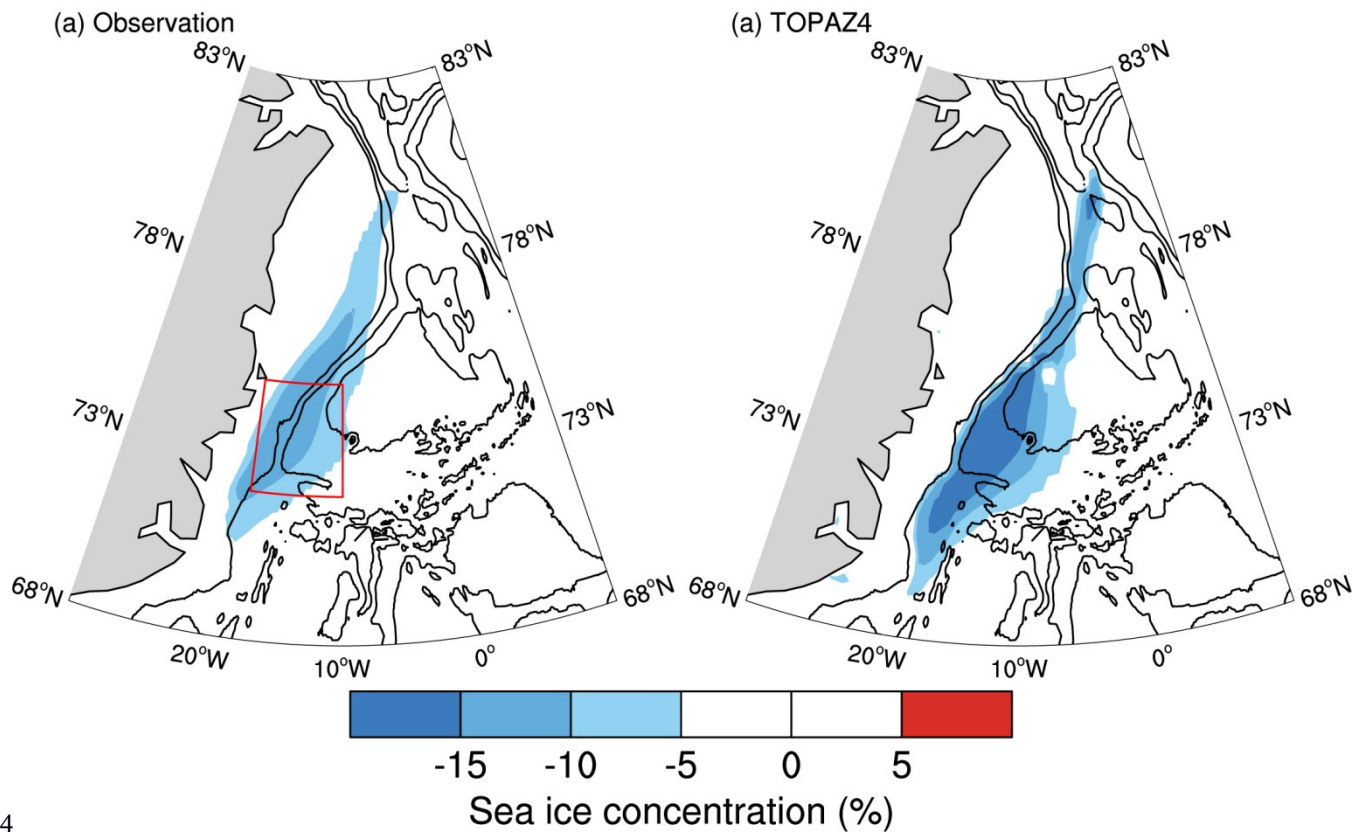
169

170

171**Figure 4:** Comparison between EN4 observation (red lines) and TOPAZ4 (blue lines). Monthly mean (thin lines) and one
 172year running mean (thick lines) of potential temperature (a,c), salinity (b,d) and stratification index (e, difference of potential
 173density between 200m and surface) averaged over 72 N:75 N; 18 W:10 W in the south-western GS as marked in Fig. 2. (a,b)
 174are for 0-50m depth average and (c,d) for 100-400m depth average. (f) DJF mean sea ice concentration in the same region
 175from satellite observation (red) and TOPAZ4 (blue).

1773. Results

178The regression map of winter mean SIC on the gyre index showed significant negative SIC in the south-western GS (Fig. 5).
179The spatial pattern of the regression coefficients closely resembles the standard deviation of winter mean SIC in the GS, as
180shown in Fig. 2. This indicates that a considerable amount of the SIC variability in GS can be associated with GSG
181circulation. However, it should be noted that the atmospheric forcing in the NS can influence both the GSG circulation
182(Aagaard 1970; Legutke 2002; Chatterjee et al. 2018) and SIC variability in the GS (Germe et al. 2011).



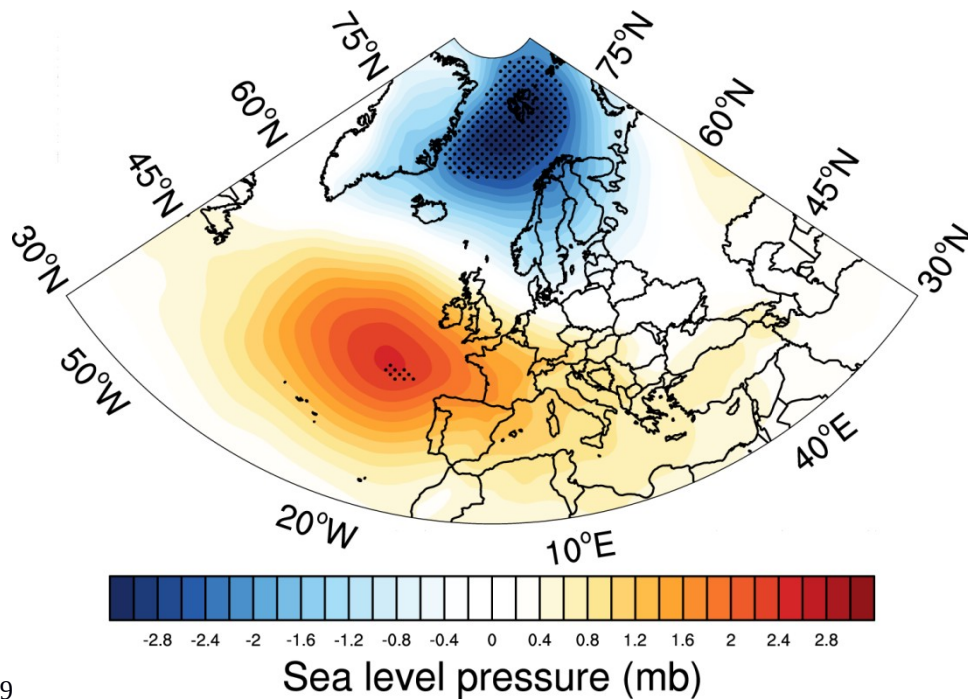
184

185

186

187 **Figure 5:** Linear regression of winter mean (DJF) sea ice concentration from (a) satellite observation (b) TOPAZ reanalysis
 188 on the gyre index. Only significant values at 95 % level are shown. Contours are bottom topography drawn at every 1000 m.

189 To elucidate the possible influence of atmospheric circulation pattern associated with GSG circulation on the SIC variability
 190 in the GS, linear regression of the sea level pressure anomalies on the gyre index was calculated and shown in Fig. 6. The
 191 large-scale atmospheric circulation shows a positive NAO-like pattern associated with a strong GSG circulation, but with
 192 centres of actions north of their usual locations (Fig. 6). The GSG circulation responds to the anomalous wind stress curl
 193 induced by the low SLP anomaly patterns in the NS (Chatterjee et al. 2018). However, we found that the station based NAO
 194 index, with its spatial feature highlighting the Icelandic low and Azores high, (https://climatedataguide.ucar.edu/sites/default/files/nao_station_seasonal.txt) and the gyre index have a very low correlation ($r = 0.2$). This further points to the importance
 196 of the spatial variability of NAO (Zhang et al. 2008; Moore et al. 2012) and its influence on the Nordic Seas circulation.
 197 Also note that the low correlation could be due to the fact that the equatorward pole of NAO doesn't exhibit much significant
 198 regression patterns in Fig. 6.

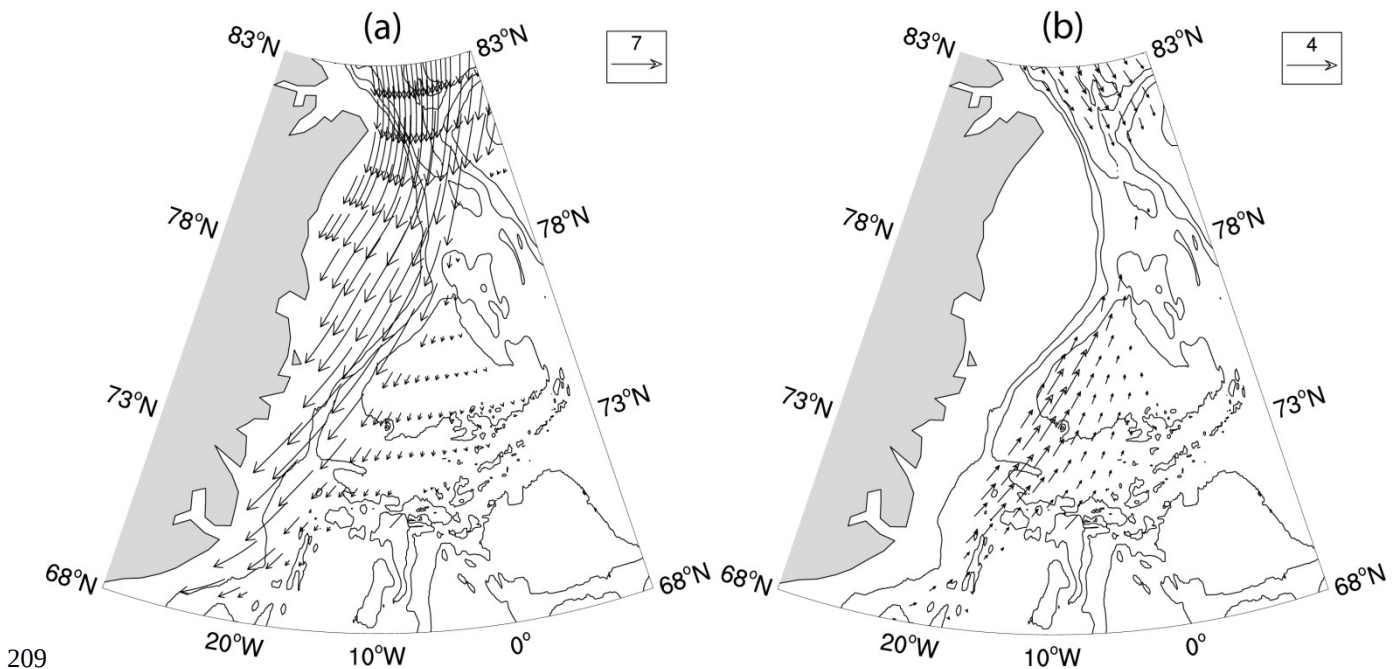


199

200 **Figure 6:** Linear regression of DJF mean sea level pressure anomaly on the gyre index. Regions with 95% statistical
 201 significance are dotted.

202 The mean southward sea ice export in the GS across the FS (Fig 7a) is strongly driven by the geostrophic winds in this
 203 region (Smedsrud et al. 2017). The low SLP pattern over NS associated with the GSG circulation can induce anomalous
 204 northerlies in GS. Linear regression of sea ice velocities on the gyre index showed anomalous northward sea ice velocities in
 205 GS associated with increase in GSG strength (Fig. 7b). This indicates that the anomalous northerly winds during a strong
 206 GSG circulation would lead to Ekman drift of sea ice which tends to push the sea ice towards the Greenland coast and reduce

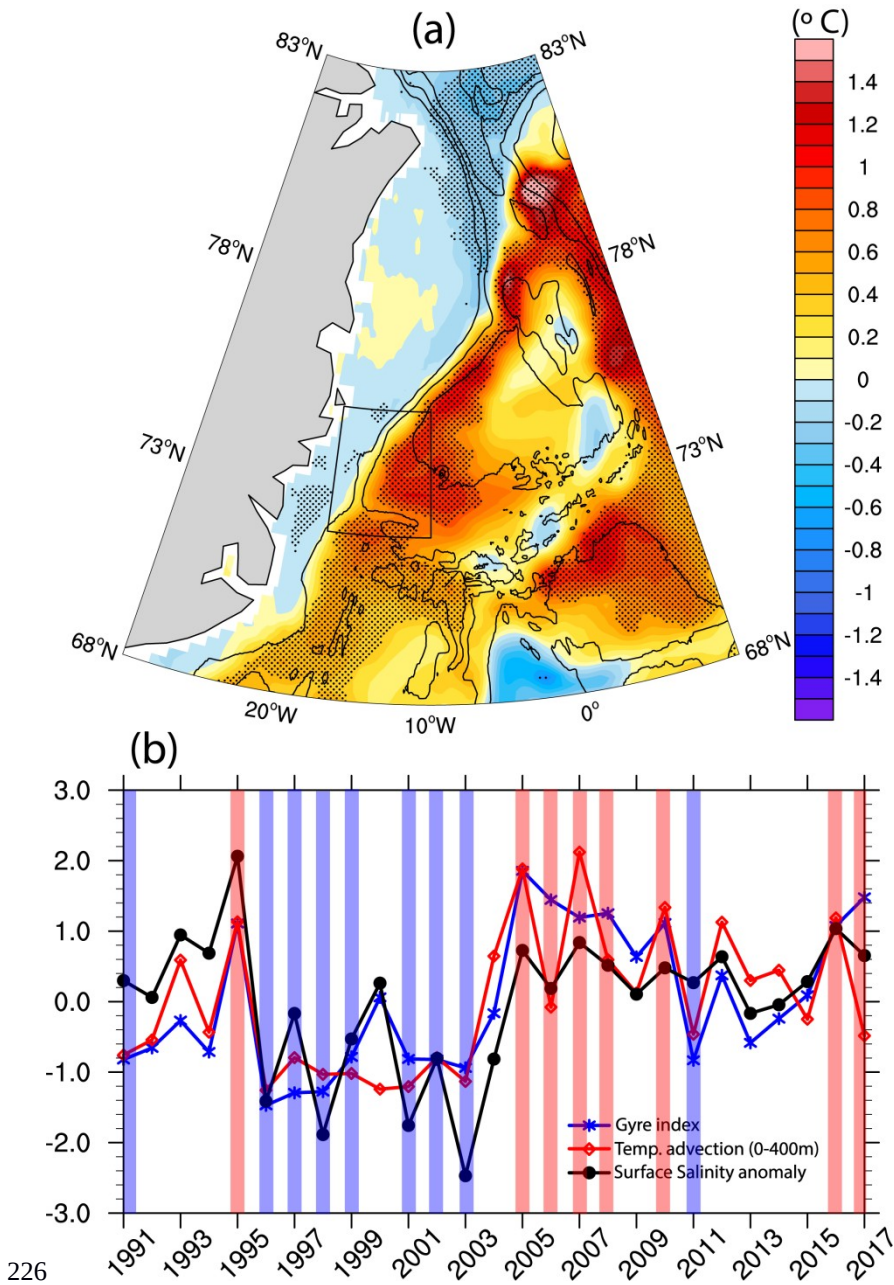
207the mean southward sea ice velocities in this region (Fig. 7a). This could lead to reduced sea ice export in this region and
 208result in low SIC.



209

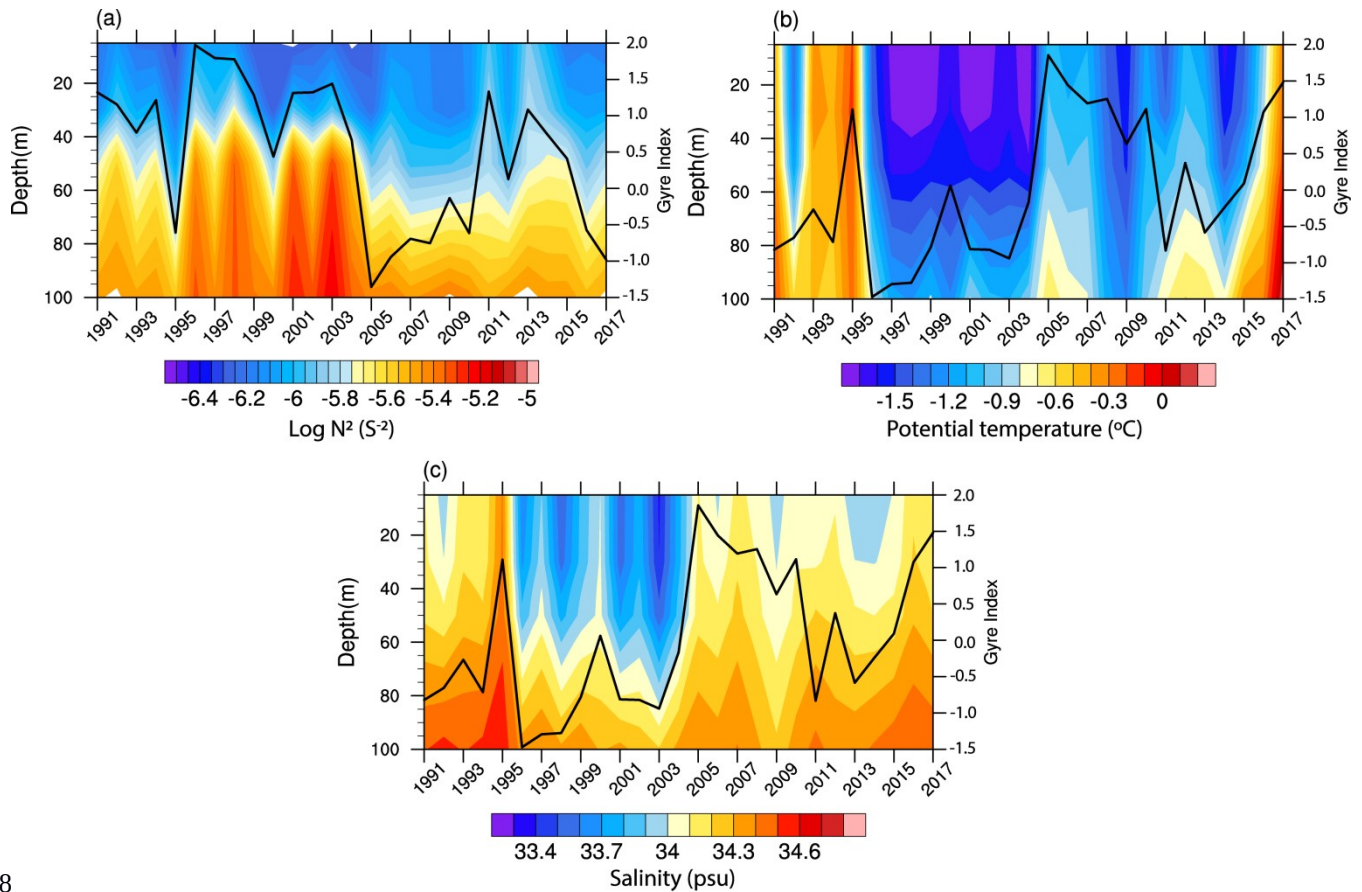
210
 211**Figure 7:** (a) Climatological (1991–2017) DJF sea ice velocity vectors (cm/s) from satellite observations. (b) Regression of
 212DJF sea ice velocity anomalies (cm/s) on the gyre index. Only results significant at 95 % are shown for clarity. Contours are
 213bottom topography drawn at every 1000 m.

214Next, we investigate GSG’s potential in influencing the oceanic conditions and hence the sea ice in the GS, given that the
 215local oceanic conditions largely affect the sea ice conditions therein (Johannessen et al. 1987; Visbeck et al. 1995; Kern et al.
 2162010; Selyuzhenok et al. 2020). Figure 8a shows the difference in ocean temperature anomaly in the upper 400m averaged
 217for the strong and weak GSG circulation years (marked in Fig 8b; see methods for definitions). The average temperature
 218anomaly for the strong GSG circulation years was found to be $\sim 1^\circ\text{C}$ higher than the same during weak GSG circulation
 219years. The warm anomalies further extend eastward with the JMC towards the central GS and could potentially affect the sea
 220ice formation in the Odden region. Further, we found significant positive correlation ($r=0.7$, $p<0.01$; Fig 8b) between gyre
 221index and temperature advection ($U \cdot \nabla T$ in upper 400m) in the south-western GS (marked region in Fig. 8a), where
 222maximum GSG influence on SIC is found (Fig. 3a). This suggests that a strong GSG circulation recirculates the warm AW
 223anomalies into the south-western GS from the FS. This is consistent with earlier study indicating an increased oceanic heat
 224content in the south-western GS due to a stronger GSG circulation (Chatterjee et al., 2018).



227**Figure 8:** (a) Difference between 400 m depth averaged potential temperature anomalies ($^{\circ}\text{C}$) averaged for strong (red bars
 228in (b)) and weak (blue bars in (b)) gyre index years. (b) Gyre index (blue), and standardized surface salinity anomaly (black),
 229temperature advection ($U \cdot \nabla T$) in upper 400 m (red) for DJF over the region 72 N : 75 N; 18 W : 10 W, as marked in (a).

230 However, it should be noted that the recirculated AW in the GS still remains dense enough to be in subsurface (Schlichtholz
 231 & Houssais 1999; Eldevik et al. 2009) and needs to be vertically mixed to have an impact on the sea ice. We found that the
 232 upper ocean stratification in the south-western GS strongly covaries with GSG circulation strength (Fig. 9a). The analysis
 233 shows that a weakening of the stratification in the upper part of the water column coincides with a stronger GSG circulation
 234 and vice versa (Fig. 9a). Further, warm and saline signatures in the upper ocean can be found during strong GSG circulation,
 235 indicating enhanced vertical mixing of the AW in the south-western GS (Figs. 9b,c). This is further confirmed by significant
 236 positive correlation ($r=0.7$, $p<0.01$) between surface salinity anomaly and gyre index (Fig. 8b). These surface anomalies can
 237 further inhibit new sea ice formation and also may cause melting of existing sea ice from the bottom.



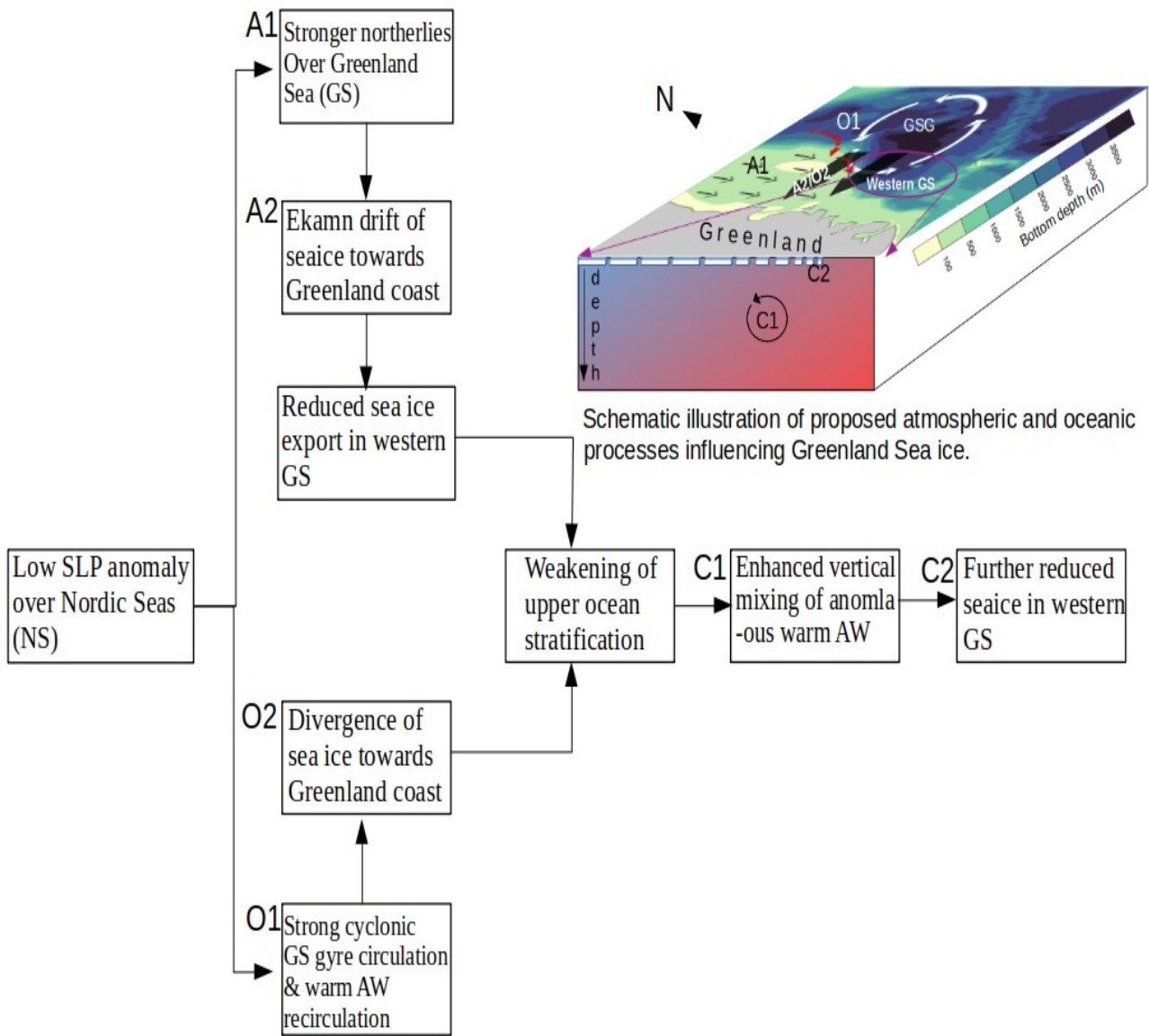
238

239

240 **Figure 9:** (a) Logarithm of squared Brunt-Väisälä Frequency (N^2 , colour shaded) (b) potential temperature (c) salinity for
 241 DJF over the region 72 N:75 N; 18 W:10 W, as marked in Figure 8a. The black timeseries against the right Y axis is the gyre
 242 index in all three panels. Note that the gyre index is plotted against a reversed Y axis in (a) for ease of comparison.

2444. **Discussions and Conclusions**

245Here we investigated the combined influence of atmospheric and oceanic circulations on the interannual variability of the
246winter mean SIC variability in the GS and showed that NS, in particular the GSG circulation can significantly contribute to
247the SIC variability in south-western GS. Fig. 10 shows the flow chart and a schematic illustration of the mechanisms
248proposed in this study. The large-scale atmospheric circulation pattern that influences the GSG circulation resembles a
249NAO-like pattern with its northern centre of action situated northeast of the typical NAO pattern. The cyclonic GSG
250circulation strengthens in response to the positive wind stress curl induced by the low SLP anomaly in the NS (Legutke
2512002, Chatterjee et al. 2018). The resulting northerly wind anomalies over GS can potentially alter the sea ice export across
252the FS (Kwok & Rothrock 1999; Jung & Hilmer 2001; Vinje 2001; Tsukernik et al. 2010; Smedsrud et al. 2011; Ionita et al.
2532016). However, winter mean SIC in the GS and FS ice area flux are not strongly correlated (Kwok et al., 2004; Germe et
254al., 2011), suggesting that the SIC variability in the GS can be significantly influenced by the local sea ice dynamics and
255oceanic conditions.



256

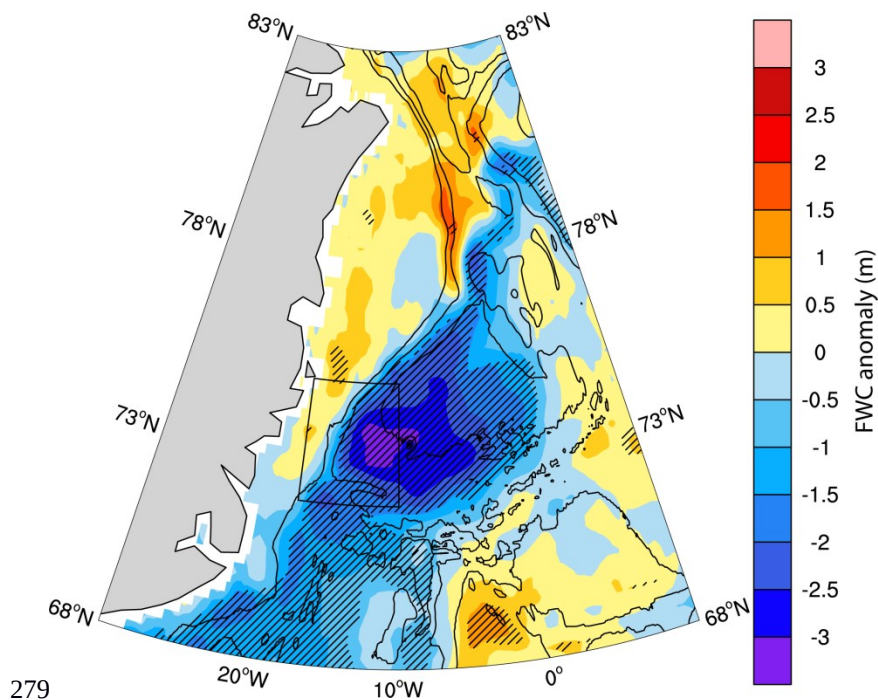
257

258

259 **Figure 10:** A flow chart and schematic diagram of the proposed processes influencing the SIC variability in the south-
 260 western GS.

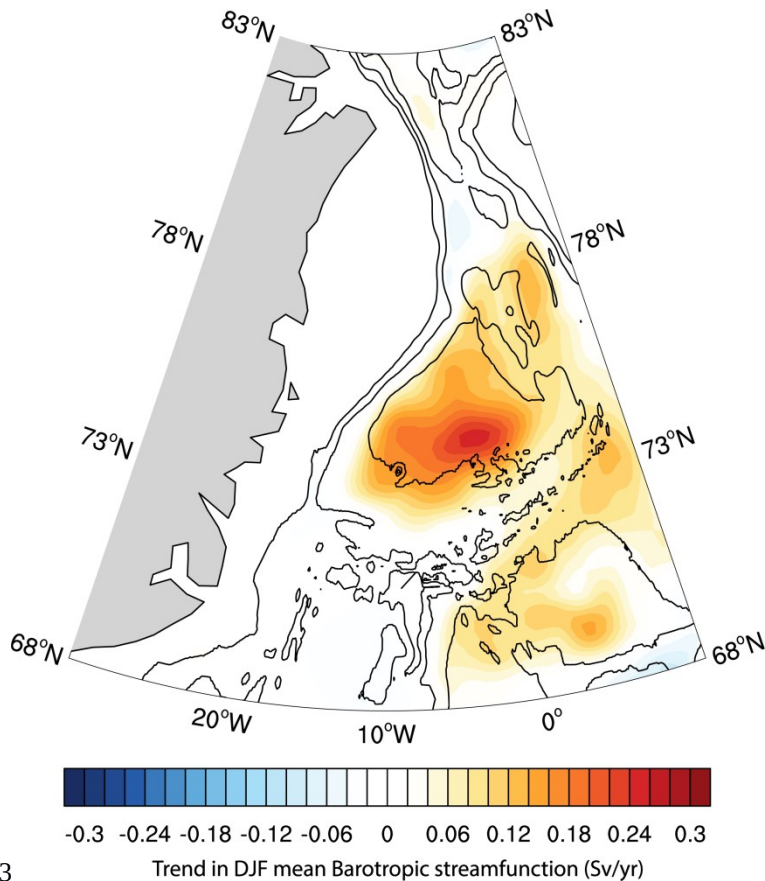
261

262 Anomalous winds in the Nordic Seas are known to influence the SIC in the GS through Ekman drift of the sea ice (Germe et al., 2011). During time-periods with anomalously low SLP over NS, anomalous northerly winds and associated Ekman drift towards the Greenland coast that can reduce the sea ice export in the western and central GS (Fig 8b). Enhanced Ekman divergence due to a strengthened GSG circulation can further lead to reduced freshwater and sea ice in the south-western GS (Fig. 11). We found that these can lead to weakening of the upper ocean stratification in the south-western GS (Fig. 9a). At the same time, a stronger GSG circulation recirculates the warm and saline subsurface AW anomalies from the FS into the south-western GS (Fig 8a). These AW anomalies can warm the surface waters by enhanced vertical mixing in a weakly stratified condition (Fig. 9) and can cause further reduction of SIC by inhibiting new sea ice formation or even melting the sea ice from bottom. Although our study doesn't show bottom melting of the sea ice, this can be realized from the findings by Ivanova et al. (2011) which showed enhanced bottom melting in this region during positive NAO periods. Thus, the SIC variability in the south-western GS responds to simultaneous influences from the atmospheric and oceanic circulation (Fig. 10). Despite the known influences of smaller scale processes, such as eddies and wave interactions on the SIC in the south-western GS, our results show that the larger scale processes can also significantly affect the SIC variability in the region, particularly on interannual timescales when the impacts of smaller scale processes can cancel out or may not be strong enough to dampen the impact of larger scale processes. However, as found in Raj et al., (2020) interactions between the gyre circulation and the eddies can be an important factor controlling the oceanic conditions and hence the SIC in the south-western GS.



280 **Figure 11:** Difference in freshwater content (FWC) anomaly (m) between strong and weak gyre index periods. Significant
281 differences at 95% level are stippled.

282



287

288 This study finds one of the mechanisms of SIC variability in the GS, highlighting the role of large scale atmospheric and
289 oceanic circulations in the NS. Observations and modelling results suggest stronger atmospheric forcing in the NS due to
290 spatial variation of the NAO (Zhang et al. 2008) and its tendency towards positive phase in a warmer climate (Bader et al.
291 2011; Stephenson et al. 2016). Consistent with that we find a significant positive trend in the GSG circulation strength
292 during the study period (Fig. 12). The response of GSG circulation to this altered atmospheric forcing can further be realized
293 with increased GSG strength (Fig. 1c) and a northeastward displacement of NAO's poleward centre of action in the Nordic
294 Seas during early 2000s (Fig. 1a in Zhang et al., 2008). Recent observations further suggest intensified convection in the

295GSG and changes in water mass formation during the last two decades (Lauvset et al., 2018; Brakstad et al., 2019). Lauvset
296et al., (2018) further discussed the role of recirculated AW on inducing intensified convection in the GSG through surface
297salinity anomaly. Consistent with this, our results show that the salinity anomalies and intensified convection in the GSG can
298be induced by a stronger GSG circulation (in response to the atmospheric forcing) which helps in recirculation of AW
299anomalies in the GS. Thus we propose that the atmospheric forcing over the NS imposes a positive oceanic feedback (Fig.
30013). The low SLP anomaly over the NS strengthens the GSG circulation. The Ekman divergence pushes the freshwater and
301sea ice from the GS interior towards the coast. Enhanced AW recirculation due to a stronger GSG and weakened
302stratification due to reduced freshwater allows the warm and saline AW anomalies to get vertically mixed and increase the
303temperature and salinity in the central GS. The increased salinity further helps in a stronger GSG circulation, completing the
304feedback loop. However it should be noted that the complex subsurface processes and their interactions with large scale
305circulation are often difficult to capture in the reanalysis, particularly with sparse and interrupted subsurface observations
306over time and space. For example, while the surface variables are well captured in TOPAZ4, it has some limitations with the
307subsurface properties as observed in Xie et. al, 2017. Of particular interest in this study, the south-south-western GS, is an
308exceptionally observational data sparse region. Increased long-term observations from these areas will be helpful in
309improvement of the reanalysis datasets and better understanding of the complex atmosphere-ocean interaction processes and
310their impact on the sea ice variability of this region.

311

312

313

314

315

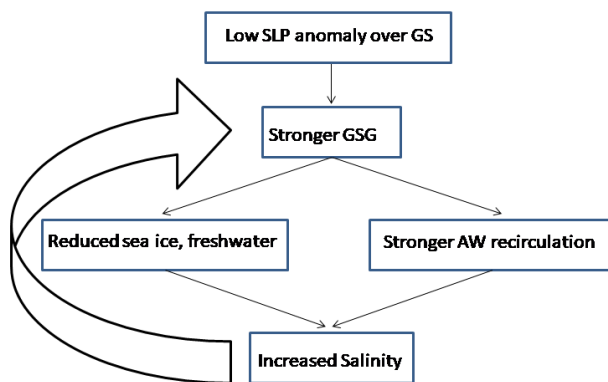
316

317

318

319

320



321**Figure 13:** A proposed positive oceanic feedback induced by atmospheric forcing in NS.

322

323**Acknowledgments**

324Sea ice concentration (<https://nsidc.org/data/NSIDC-0051/versions/1>) and velocity
325(<https://nsidc.org/data/nsidc-0116/versions/4>) are obtained from the National Snow and Ice Data Centre. The TOPAZ4
326simulations have used grants of computing time (nn2993k) and storage (ns2993k) from the Sigma2 infrastructure. The
327monthly TOPAZ4 results used in this study are obtained via CMEMS (marine.copernicus.eu). EN4 (version 4.2.1)
328observational data is provided by UK Met Office Hadley Centre and obtained from
329<https://www.metoffice.gov.uk/hadobs/en4/download-en4-2-1.html>. Authors thank Ola M Johannessen, Nansen Scientific
330Society for valuable suggestions during the course of the study. NCPOR is an autonomous institute fully funded by
331Ministry of Earth Sciences, Govt. of India. This is NCPOR contribution number J-97/2020-21. All figures were made using
332The NCAR Command Language (Version 6.4.0).

333

334**Declarations**

335**Funding** (information that explains whether and by whom the research was supported)

336Not Applicable

337**Conflicts of interest/Competing interests** (include appropriate disclosures)

338Authors declare no Conflicts of interest/Competing interests

339**Availability of data and material** (data transparency)

340All the data used here are freely available on respective data portals (links provided in the ‘Acknowledgements’ section)

341**Code availability (software application or custom code)**

342All the codes are available on reasonable request to the corresponding author.

343**Authors' contributions**

344SC conceived the idea in discussion with RPR and wrote the manuscript. SC performed all the analyses. All authors
345contributed in improvement and writing of the manuscript.

346

347

348

349

350

351

352**References**

353Aagaard, K.: Wind-driven transports in the Greenland and Norwegian seas, Deep. Res. Oceanogr. Abstr., doi:10.1016/0011-
3547471(70)90021-5, 1970.

355Aagaard, K. and Carmack, E. C.: The role of sea ice and other fresh water in the Arctic circulation, J. Geophys. Res.,
356doi:10.1029/jc094ic10p14485, 1989.

357Bader, J., Mesquita, M. D. S., Hodges, K. I., Keenlyside, N., Østerhus, S. and Miles, M.: A review on Northern Hemisphere
358sea-ice, storminess and the North Atlantic Oscillation: Observations and projected changes, *Atmos. Res.*,
359doi:10.1016/j.atmosres.2011.04.007, 2011.

360Belkin, I. M., Levitus, S., Antonov, J. and Malmberg, S. A.: “Great Salinity Anomalies” in the North Atlantic, *Prog.*
361*Oceanogr.*, doi:10.1016/S0079-6611(98)00015-9, 1998.

362Bourke, R. H., Paquette, R. G. and Blythe, R. F.: The Jan Mayen Current of the Greenland Sea, *J. Geophys. Res.*,
363doi:10.1029/92jc00150, 1992.

364Brakstad, A., K. Våge, L. Håvik, and G. W. K. Moore, 2019: Water Mass Transformation in the Greenland Sea during the
365Period 1986–2016. *J. Phys. Oceanogr.*, 49, 121–140, <https://doi.org/10.1175/JPO-D-17-0273.1>.

366

367Campbell, W. J., Gloersen, P., Josberger, E. G., Johannessen, O. M., Guest, P. S., Mognard, N., Shuchman, R., Burns, B. A.,
368Lannelongue, N. and Davidson, K. L.: Variations of mesoscale and large-scale sea ice morphology in the 1984 marginal ice
369zone experiment as observed by microwave remote sensing, *J. Geophys. Res. Ocean.*, doi:10.1029/JC092iC07p06805, 1987.

370Cavalieri, D.J., Parkinson, C. L., Gloersen, P. & Zwally H. J.: Sea Ice Concentrations From Nimbus-7 SMMR and DMSP
371SSM/I Passive Microwave Data, Natl. Snow and Ice Data Cent., Boulder, Colorado, 1996 [Updated 2018].

372Chafik L., and Rossby T.: Volume, heat, and freshwater divergences in the Subpolar North Atlantic suggest the Nordic Seas
373as key to the state of the Meridional Overturning Circulation. *Geophysical Research Letters* 46: doi:10.1029/2019GL082
374110. 2019

375Chatterjee, S., Raj, R. P., Bertino, L., Skagseth, Ravichandran, M. and Johannessen, O. M.: Role of Greenland Sea Gyre
376Circulation on Atlantic Water Temperature Variability in the Fram Strait, *Geophys. Res. Lett.*, doi:10.1029/2018GL079174,
3772018.

378Comiso, J. C., Wadhams, P., Pedersen, L. T. and Gersten, R. A.: Seasonal and interannual variability of the Odden ice
379tongue and a study of environmental effects, *J. Geophys. Res. Ocean.*, doi:10.1029/2000jc000204, 2001.

380

381

382Dee, D. P., Uppala, S. M., Simmons, A. J., Berrisford, P., Poli, P., Kobayashi, S., Andrae, U., Balmaseda, M. A., Balsamo,
383G., Bauer, P., Bechtold, P., Beljaars, A. C. M., van de Berg, L., Bidlot, J., Bormann, N., Delsol, C., Dragani, R., Fuentes, M.,
384Geer, A. J., Haimberger, L., Healy, S. B., Hersbach, H., Hólm, E. V., Isaksen, L., Kållberg, P., Köhler, M., Matricardi, M.,
385Mcnally, A. P., Monge-Sanz, B. M., Morcrette, J. J., Park, B. K., Peubey, C., de Rosnay, P., Tavolato, C., Thépaut, J. N. and

386Vitart, F.: The ERA-Interim reanalysis: Configuration and performance of the data assimilation system, *Q. J. R. Meteorol.*
387*Soc.*, doi:10.1002/qj.828, 2011.

388Deser, C., Walsh, J. E. and Timlin, M. S.: Arctic sea ice variability in the context of recent atmospheric circulation trends, *J.*
389*Clim.*, doi:10.1175/1520-0442(2000)013<0617:ASIVIT>2.0.CO;2, 2000.

390Dickson, R. R., Meincke, J., Malmberg, S. A. and Lee, A. J.: The “great salinity anomaly” in the Northern North Atlantic
3911968-1982, *Prog. Oceanogr.*, doi:10.1016/0079-6611(88)90049-3, 1988.

392

393Eldevik, T., Nilsen, J. E., Iovino, D., Anders Olsson, K., Sandø, A. B. and Drange, H.: Observed sources and variability of
394Nordic seas overflow, *Nat. Geosci.*, doi:10.1038/ngeo518, 2009.

395Germe, A., Houssais, M. N., Herbaut, C. and Cassou, C.: Greenland Sea sea ice variability over 1979-2007 and its link to the
396surface atmosphere, *J. Geophys. Res. Ocean.*, 116(10), 1–14, doi:10.1029/2011JC006960, 2011.

397Grebmeier, J. M., Smith, W. O. and Conover, R. J.: Biological processes on Arctic continental shelves: Ice-ocean-biotic
398interactions., 2011.

399Hattermann, T., Isachsen, P. E., Von Appen, W. J., Albretsen, J. and Sundfjord, A.: Eddy-driven recirculation of Atlantic
400Water in Fram Strait, *Geophys. Res. Lett.*, doi:10.1002/2016GL068323, 2016.

401Hilmer, M. and Jung, T.: Evidence for a recent change in the link between the North Atlantic Oscillation and Arctic sea ice
402export, *Geophys. Res. Lett.*, doi:10.1029/1999GL010944, 2000.

403Huang, J., Pickart, R.S., Huang, R.X., Lin, P., Brakstad, A. and Xu, F.: Sources and upstream pathways of the densest
404overflow water in the Nordic Seas. *Nat Commun.*, <https://doi.org/10.1038/s41467-020-19050-y>, 2020.

405Hunke, E. C. and Dukowicz, J. K.: An elastic-viscous-plastic model for sea ice dynamics, *J. Phys. Oceanogr.*, 27, 1849–
4061867, 1997.

407Hurrell, J. W.: Decadal trends in the North Atlantic oscillation: Regional temperatures and precipitation, *Science* (80-.),
408doi:10.1126/science.269.5224.676, 1995.

409Instanes, A., Anisimov, O., Brigham, L., Goering, D., Khrustalev, L. N., Ladanyi, B., Larsen, J. O., Smith, O., Stevermer,
410A., Weatherhead, B. and Weller, G.: Infrastructure: buildings, support systems, and industrial facilities, in *Arctic Climate*
411*Impact Assessment.*, 2005.

412Ionita, M., Scholz, P., Lohmann, G., Dima, M. and Prange, M.: Linkages between atmospheric blocking, sea ice export
413through Fram Strait and the Atlantic Meridional Overturning Circulation, *Sci. Rep.*, doi:10.1038/srep32881, 2016.

- 414Jeansson, E., Olsen, A. and Jutterström, S.: Arctic Intermediate Water in the Nordic Seas, 1991–2009, Deep. Res. Part I
415Oceanogr. Res. Pap., doi:10.1016/j.dsr.2017.08.013, 2017.
- 416Johannessen, O. M., Johannessen, J. A., Svendsen, E., Shuchman, R. A., Campbell, W. J. and Josberger, E.: Ice-edge eddies
417in the Fram Strait marginal ice zone, Science (80-.), doi:10.1126/science.236.4800.427, 1987.
- 418Johannessen, O. M., Bengtsson, L., Miles, M. W., Kuzmina, S. I., Semenov, V. A., Alekseev, G. V., Nagurnyi, A. P.,
419Zakharov, V. F., Bobylev, L. P., Pettersson, L. H., Hasselmann, K. and Cattle, H. P.: Arctic climate change: Observed and
420modelled temperature and sea-ice variability, Tellus, Ser. A Dyn. Meteorol. Oceanogr., doi:10.1111/j.1600-
4210870.2004.00060.x, 2004.
- 422Jung, T. and Hilmer, M.: The link between the North Atlantic oscillation and Arctic sea ice export through Fram Strait, J.
423Clim., doi:10.1175/1520-0442(2001)014<3932:TLBTNA>2.0.CO;2, 2001.
- 424Kern, S., Kaleschke, L. and Spreen, G.: Climatology of the nordic (irminger, greenland, barents, kara and white/pechora)
425seas ice cover based on 85 GHz satellite microwave radiometry: 1992-2008, Tellus, Ser. A Dyn. Meteorol. Oceanogr.,
426doi:10.1111/j.1600-0870.2010.00457.x, 2010.
- 427Killworth, P. D.: On “Chimney” Formations in the Ocean, J. Phys. Oceanogr., doi:10.1175/1520-
4280485(1979)009<0531:ofito>2.0.co;2, 1979.
- 429
- 430Kwok, R.: Fram Strait sea ice outflow, J. Geophys. Res., 109(C1), C01009, doi:10.1029/2003JC001785, 2004.
- 431Kwok, R. and Rothrock, D. A.: Variability of Fram Strait ice flux temperature 2 , -7 % of the area of the Arctic Ocean . The
432winter area flux ranges from a minimum to a maximum of October May 1995 is 1745 km from a low of 1375 km the 1990
433flux to a high of 2791 km The sea level pressu, J. Geophys. Res., 104(1998), 5177–5189, 1999.
- 434Kwok, R., Cunningham, G. F., Wensnahan, M., Rigor, I., Zwally, H. J. and Yi, D.: Thinning and volume loss of the Arctic
435Ocean sea ice cover: 2003-2008, J. Geophys. Res. Ocean., doi:10.1029/2009JC005312, 2009.
- 436Lauvset, S.K., Brakstad, A., Våge, K., Olsen, A., Jeansson, E., Mork, K.A.: Continued warming, salinification and
437oxygenation of the Greenland Sea gyre, Tellus A, 70 (1), pp.1-9, doi:10.1080/16000870.2018.1476434, 2018.
- 438Legutke, S.: A Numerical Investigation of the Circulation In the Greenland and Norwegian Seas, J. Phys. Oceanogr.,
439doi:10.1175/1520-0485(1991)021<0118:aniotc>2.0.co;2, 2002.
- 440Levitus et al.: Global ocean heat content 1955-2008 in light of recently revealed instrumentation problems. Geophysical
441Research Letters, 36, L07608. doi:<http://dx.doi.org/10.1029/2008GL037155>, 2009

442Lien, V. S., Hjøllø, S. S., Skogen, M. D., Svendsen, E., Wehde, H., Bertino, L., Counillon, F., Chevallier, M. and Garric, G.:
443An assessment of the added value from data assimilation on modelled Nordic Seas hydrography and ocean transports, *Ocean*
444*Model.*, doi:10.1016/j.ocemod.2015.12.010, 2016.

445Lind, S., Ingvaldsen, R. B. and Furevik, T.: Arctic warming hotspot in the northern Barents Sea linked to declining sea-ice
446import, *Nat. Clim. Chang.*, doi:10.1038/s41558-018-0205-y, 2018.

447Marshall, J. and Schott, F.: Open-ocean convection: Observations, theory, and models, *Rev. Geophys.*,
448doi:10.1029/98RG02739, 1999.

449Moore, G. W. K., Renfrew, I. A. and Pickart, R. S.: Multidecadal mobility of the north atlantic oscillation, *J. Clim.*,
450doi:10.1175/JCLI-D-12-00023.1, 2013.

451

452Nansen, F.: Blant Sel og Bjørn. Min første Ishavs-Ferd [With Seals and Bears: My First Journey to the Arctic Seas], Jacob
453Dybwads Forlag, Oslo, 285 pp, 1924.

454Raj, R. P., Chatterjee, S., Bertino, L., Turiel, A. & Portabella, M.: The Arctic Front and its variability in the Norwegian Sea,
455*Ocean Sci.*, 15, 1729–1744, <https://doi.org/10.5194/os-15-1729-2019>, 2019.

456Raj, R. P., Halo, I., Chatterjee, S., Belonenko, T., Bakhoday Paskyabi, M., Bashmachnikov, I., Federov, A., Xie P. :
457Interaction between mesoscale eddies and the gyre circulation in the Lofoten Basin. *Journal of Geophysical Research:*
458*Oceans*, 125, e2020JC016102. <https://doi.org/10.1029/2020JC016102>, 2020.

459Rogers, J. C., and Hung, M. P. (2008), The Odden ice feature of the Greenland Sea and its association with atmospheric
460pressure, wind, and surface flux variability from reanalyses, *Geophys. Res. Lett.*, 35, L08504, doi:10.1029/2007GL032938.

461Sakov, P., Counillon, F., Bertino, L., Lister, K. A., Oke, P. R. and Korabely, A.: TOPAZ4: An ocean-sea ice data
462assimilation system for the North Atlantic and Arctic, *Ocean Sci.*, doi:10.5194/os-8-633-2012, 2012.

463Schott, F., Visbeck, M. and Fischer, J.: Observations of vertical currents and convection in the central Greenland Sea during
464the winter of 1988-1989, *J. Geophys. Res.*, doi:10.1029/93jc00658, 1993.

465Selyuzhenok, V., Bashmachnikov, I., Ricker, R., Vesman, A. & Bobylev, L.: Sea ice volume variability and water
466temperature in the Greenland Sea, *The Cryosphere*, 14, 477–495, <https://doi.org/10.5194/tc-14-477-2020>, 2020.

467Serreze, M. C., Barrett, A. P., Slater, A. G., Woodgate, R. A., Aagaard, K., Lammers, R. B., Steele, M., Moritz, R.,
468Meredith, M. and Lee, C. M.: The large-scale freshwater cycle of the Arctic, *J. Geophys. Res. Ocean.*,
469doi:10.1029/2005JC003424, 2006.

470

471Shuchman, R. A., Josberger, E. G., Russel, C. A., Fischer, K. W., Johannessen, O. M., Johannessen, J. and Gloersen, P.:
472Greenland Sea Odden sea ice feature: Intra-annual and interannual variability, *J. Geophys. Res. Ocean.*,
473doi:10.1029/98jc00375, 1998.

474Smedsrud, L. H., Sirevaag, A., Kloster, K., Sorteberg, A. and Sandven, S.: Recent wind driven high sea ice area export in the
475Fram Strait contributes to Arctic sea ice decline, *Cryosphere*, doi:10.5194/tc-5-821-2011, 2011.

476Stephenson, D. B., Pavan, V., Collins, M., Junge, M. M. and Quadrelli, R.: North Atlantic Oscillation response to transient
477greenhouse gas forcing and the impact on European winter climate: A CMIP2 multi-model assessment, *Clim. Dyn.*,
478doi:10.1007/s00382-006-0140-x, 2006.

479Toudal, L.: Ice extent in the Greenland Sea 1978-1995, *Deep. Res. Part II Top. Stud. Oceanogr.*, doi:10.1016/S0967-
4800645(99)00021-1, 1999.

481Tschudi, M., Meier, W. N., Stewart, J. S., Fowler, C. & Maslanik, J.: Polar Pathfinder Daily 25 km EASE-Grid Sea Ice
482Motion Vectors, Version 4. Boulder, Colorado USA. NASA National Snow and Ice Data Center Distributed Active Archive
483Center. Doi: <https://doi.org/10.5067/INAWUWO7QH7B>. 2019. [Updated 2019]

484Tsukernik, M., Deser, C., Alexander, M. and Tomas, R.: Atmospheric forcing of Fram Strait sea ice export: A closer look,
485*Clim. Dyn.*, 35(7), 1349–1360, doi:10.1007/s00382-009-0647-z, 2010.

486Våge, K., Papritz, L., Håvik, L., Spall, M. A. and Moore, G. W. K.: Ocean convection linked to the recent ice edge retreat
487along east Greenland, *Nat. Commun.*, doi:10.1038/s41467-018-03468-6, 2018.

488Vinje, T.: Fram Strait Ice Fluxes and Atmospheric Circulation: 1950-2000, *J. Clim.*, doi:10.1175/1520-
4890442(2001)014<3508:FSIFAA>2.0.CO;2, 2001.

490Visbeck, M., Fischer, J. and Schott, F.: Preconditioning the Greenland Sea for deep convection: ice formation and ice drift, *J.*
491*Geophys. Res.*, doi:10.1029/95jc01611, 1995.

492Wadhams, P. and Comiso, J. C.: Two modes of appearance of the Odden ice tongue in the Greenland Sea, *Geophys. Res.*
493*Lett.*, doi:10.1029/1999GL900502, 1999.

494Wadhams, P., Comiso, J. C., Prussen, E., Wells, S., Brandon, M., Aldworth, E., Viehoff, T., Allegrino, R. and Crane, D. R.:
495The development of the Odden ice tongue in the Greenland Sea during winter 1993 from remote sensing and field
496observations, *J. Geophys. Res. C Ocean.*, 101(C8), 18213–18235, doi:10.1029/96JC01440, 1996.

497Xie, J., Bertino, L., Knut, L. and Sakov, P.: Quality assessment of the TOPAZ4 reanalysis in the Arctic over the period
4981991-2013, *Ocean Sci.*, doi:10.5194/os-13-123-2017, 2017.

499Zamani, B., Krumpen, T., Smedsrud, L. H. and Gerdes, R.: Fram Strait sea ice export affected by thinning: comparing high-
500resolution simulations and observations, *Clim. Dyn.*, doi:10.1007/s00382-019-04699-z, 2019.

501Zhang, X., Sorteberg, A., Zhang, J., Gerdes, R. and Comiso, J. C.: Recent radical shifts of atmospheric circulations and rapid
502changes in Arctic climate system, *Geophys. Res. Lett.*, doi:10.1029/2008GL035607, 2008